Transport and Communications Science Journal, Vol. 75, Issue 1 (01/2024), 1198-1212

Transport and Communications Science Journal

ENHANCING VIBRATION CONTROL IN STAY CABLES: A MODIFIED DAMPING FORMULATION WITH NS-HDR DAMPER

Luu Xuan Le[*1], Hiroshi Katsuchi[2], Binh Xuan Luong[1], Linh Ngoc Vu[1], Quan Van Ha[1]

[1] University of Transport and Communications, No 3 Cau Giay Street, Hanoi, Vietnam

[2] Department of Civil Engineering, Yokohama National University, 79-5 Tokiwadai, Hodogaya-ku, Yokohama 240-8501, Japan

ARTICLE INFO

TYPE: Research Article
Received: 06/08/2023
Revised: 10/12/2023
Accepted: 10/01/2024
Published online: 15/01/2024
https://doi.org/10.47869/tcsj.75.1.8

[*] *Corresponding author*
Email: luusbvl@utc.edu.vn

Abstract. Cables in cable-stayed bridges have low intrinsic damping, and dampers are often used as a countermeasure for cable vibration control. This paper presents an innovative asymptotic formula for calculating the additional damping in stay cables equipped with Negative Stiffness High Damping Rubber dampers (NS-HDR). The NS-HDR damper incorporates negative stiffness through a pre-compressed spring. The analysis employs models of flexural cables with fixed-fixed or hinged-hinged ends to derive the formulation of attainable damping ratio. The results of the study reveal that the NS-HDR damper, with its negative stiffness feature, exhibits a significantly higher added damping ratio in comparison to the conventional HDR damper configuration. To quantify this increased added damping resulting from negative stiffness, a modification factor is proposed. The accuracy and effectiveness of the proposed damping formula are successfully validated using the Finite Difference Method (FDM). Subsequently, the methodology is applied to design the damping of two existing stay cables (137.82m and 167.18m in length). Field measurements reveal that the damping in these cables falls below the required threshold of 0.5%. The proposed NS-HDR damper offers a viable solution to achieve the required damping ratio. These findings contribute significantly to the understanding and optimization of damping in stay cables employing HDR dampers, presenting potential applications in the field of bridge engineering. The research opens up new possibilities for enhancing vibration control and safety in cable-stayed bridges.

Keywords: Negative stiffness HDR damper (NS-HDR); damping ratio; modification factor; field measurement.

1. INTRODUCTION

Cable systems in cable-stayed bridges are becoming more flexible, lighter and less damped, resulting in cables being more susceptible to various vibration sources, such as rain-wind induced vibration, vortex shedding, or support motions [1]. Cables without vibration controls are low-damped structures with inherently low damping ratios [2]. Gimsing and Georgakis [3] have highlighted that the inherent damping ratio of stay cables typically ranges from 0.01% to 0.20%, while the Post-Tensioning Institute Cable-Stayed Bridge Committee [4] has recommended, in their Guide Specification, a cable damping ratio (ξ) between 0.5% and 1.0% to effectively mitigate rain-wind induced vibration. Consequently, external dampers are frequently incorporated into cables to provide additional damping.

Pacheco et al. [2] proposed a universal estimation curve for the attainable damping in a taut cable with a single viscous damper, providing a convenient tool for cable damping design. Krenk [5] presented an asymptotic form of the added damping in a taut cable. Main and Jones [6, 7] subsequently addressed the limitations regarding the restriction on damper locations and vibration modes. In addition to these analytical solutions, Tabatabai and Mehrabi [8] introduced the Finite Difference Method to solve the eigenvalue equation containing the natural frequency and overall damping of a cable.

Measurements of damping in actual cables have demonstrated lower values compared to the expected ones. Recently, there has been a growing interest in studies focusing on passive vibration control using a novel negative stiffness damper (NSD) to enhance damper performance. Chen et al. [9] introduced a NSD for cable vibration control, where the NSD was constructed with a pre-compressed spring and a viscous damper. Zhou and Li [10] developed a NSD consisting of two compressed springs and an oil damper mounted on a taut cable. Other works exploring the vibration control and dynamic behavior of stay cables utilizing NSDs have been conducted, as seen in[11-13].

Conventional High Damping Rubber (HDR) dampers have been widely utilized for the vibration control of cables due to their advantages. However, the measured damping of HDR dampers often falls below theoretical values, indicating insufficient performance. To address this issue, this paper proposes the implementation of a Negative Stiffness High Damping Rubber (NS-HDR) damper to enhance damper efficiency. The damping formulation is derived using an asymptotic solution, and the improvement in added damping resulting from the negative stiffness is demonstrated through a proposed modification factor. Cable models with fixed-fixed ends or hinged-hinged ends are investigated and discussed. Additionally, a numerical approach known as the Finite Difference Method (FDM) is introduced to verify the analytically proposed damping formulation.

2. SCHEMATIC DIAGRAM

Two models of a stay cable with a negative stiffness HDR damper, namely a fixed-fixed end cable and a hinged-hinged end cable, are illustrated in Figs. 1(a) and 1(b) respectively. The cable has length l, tension T, flexural rigidity EI, and mass per unit length m. Tabatabai and Mehrabi [8] have pointed out that for the range of parameters involved in most stay cables, the influence of cable sag is insignificant whereas the cable bending stiffness can have a significant influence on the resulting cable damping ratios. For simplicity, cable sag is neglected in this analysis.

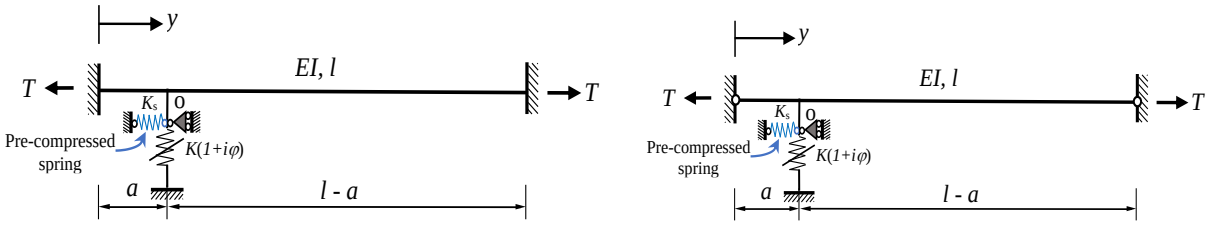

Figure 1. Cable models with a NS-HDR damper: a) fixed end cable; and b) hinged end cable.

A negative stiffness HDR damper is installed on the cable at the location $y = a$, and it is comprised of a combination of a conventional HDR damper and a pre-compressed spring. The conventional HDR damper is characterized by a damper spring factor K and a material loss factor φ. The spring has a free length l_0, an initial compressed length l_1, and a stiffness K_s. It is important to note that the spring is compressed to a certain extent to ensure that it remains in a compressed state during cable vibration. Due to this compression, the spring releases force to aid cable motion, rather than resisting it, as depicted in Fig. 2.

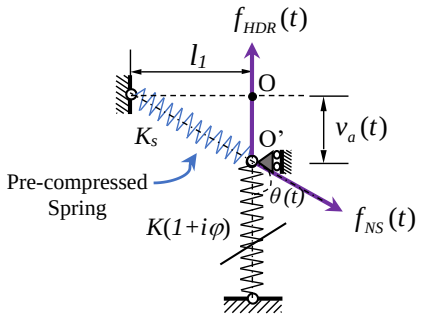

Figure. 2. Dynamic state of NS-HDR damper.

Force in the conventional HDR damper as

$$f_{HDR}(t) = K(1 + \varphi i)v_a(t) \tag{1}$$

where $i^2 = -1$; and $v_a(t)$ is the displacement of the cable at $y = a$.

Force in the spring as

$$f_{NS}(t) = K_s\left(l_0 - \sqrt{l_1^2 + v_a(t)^2}\right) \tag{2}$$

Force produced by the NS-HDR damper system is the vertical component of the force equilibrium equation.

$$f_{NSD}(t) = f_{HDR}(t) - f_{NS}(t)\cos\theta(t) \tag{3}$$

where

$$\cos\theta(t) = \frac{v_a(t)}{\sqrt{l_1^2 + v_a(t)^2}} \tag{4}$$

Eq. (3) is applied to a parallel configuration. In this parallel spring arrangement, each spring is connected to the same support structure at one end, with their opposite ends connected to a common point at the damper location. Substitution of the HDR damper force from eq. (1) and spring force from eq. (2) into eq. (3) gives

$$f_{NSD}(t) = K(1+\varphi i)v_a(t) - K_s\left(\frac{l_0}{\sqrt{l_1^2 + v_a(t)^2}} - 1\right)v_a(t) \tag{5}$$

This force of the NS-HDR damper system is nonlinear with respect to variable $v_a(t)$. This nonlinear behaviour occurs as the nonlinearity of the time-varying spring force. A damper, however, is often installed close to one cable end leading to small displacements $v_a(t)$ at a damper location. Also, by considering the compressed length of the spring $l_1 \gg v_a(t)$, eq. (5) can be linearly approximated as

$$f_{NSD}(t) = K(1+\varphi i)v_a(t) - K_s\frac{\Delta l}{l_1}v_a(t) \tag{6}$$

where $\Delta l = l_0 - l_1$ denotes the initial deformation of the compression spring. Chen et al. [9] investigated a negative stiffness viscous damper installed to a taut cable and pointed out that the nonlinear behaviour of the damper could be neglected for the practical configurations of the damper-cable system, and the linear approximation of the spring force was sufficiently accurate for damping evaluation. Denoting $K_{NS} = -K_s\Delta l/l_1$, eq. (6) becomes

$$f_{NSD}(t) = K(1+\varphi i)v_a(t) + K_{NS}v_a(t) \tag{7}$$

For the free vibration of a cable, the damper force and its displacement are in the harmonic form as

$$f_{NSD}(t) = F_{NSD}e^{i\omega t}, \text{ and } v_a(t) = \tilde{v}_a e^{i\omega t} \tag{8a,b}$$

where ω is the complex natural circular frequency of the cable; $\tilde{v}_a$ is the transverse amplitude of the cable mode shape at $y = a$; and F_{NSD} is the time-independent component of the damper force. On making use of eqs. (8a, b), eq. (7) yields

$$F_{NSD} = K_{eq}(1+\varphi_{eq}i)\tilde{v}_a \tag{9}$$

where $K_{eq} = K(1+\gamma)$ and $\varphi_{eq} = \varphi/(1+\gamma)$ characterize the equivalent spring factor and material loss factor of the HDR damper, respectively; $\bar{K}_{NS} = (K_{NS}\times a)/T$ and $\bar{K} = (K\times a)/T$ are the nondimensional forms of K_{NS} and K, correspondingly; and $\gamma = \bar{K}_{NS}/\bar{K}$.

3. DERIVATION OF ADDED DAMPING

Because of low inherent damping characteristics, the cable is considered as an undamped structure, the equation of motion of in-plane free vibration for each cable segment, $0 \le y \le a^-$ and $a^+ \le y \le l$ is derived as

$$T\frac{\partial^2 v(y,t)}{\partial y^2} - EI\frac{\partial^4 v(y,t)}{\partial y^4} - m\frac{\partial^2 v(y,t)}{\partial t^2} = 0 \tag{10}$$

where $v(y,t)$ is the transverse displacement of the cable. Noted that a^- means the left-hand side of cable's cross section at damper location while a^+ denotes the right-hand side of cable's cross section at damper location.

$$v(y,t) = \tilde{v}(y)e^{\omega i t} \tag{11}$$

Inserting eq. (11) into eq. (10) leads to

$$\eta l^2 \frac{d^4\tilde{v}(y)}{dy^4} - \frac{d^2\tilde{v}(y)}{dy^2} - \beta^2\tilde{v}(y) = 0 \tag{12}$$

where $\eta = EI/Tl^2$ is the dimensionless cable bending stiffness; and $\beta = \omega\sqrt{m/T}$ characterizes the wave number. By solving eq. (12), the mode shape of each cable segment is obtained as shown in eq. (13) and eq. (14).

For $0 \le y \le a^-$:

$$\tilde{v}_1(y) = C_1\sinh(\delta_1 y) + C_2\cosh(\delta_1 y) + C_3\sin(\delta_2 y) \; + \; C_4\cos(\delta_2 y) \tag{13}$$

For $a^+ \le y \le l$:

$$\tilde{v}_2(y) = C_5\sinh\delta_1(y-a) + C_6\cosh\delta_1(y-a) \; + \; C_7\sin\delta_2(y-a) + C_8\cos\delta_2(y-a) \tag{14}$$

where

$$\delta_{1,2} = \sqrt{\frac{\sqrt{1+4\eta l^2\beta^2}\pm 1}{2\eta l^2}} \tag{15}$$

and C_1 to C_8 are constants. These constants from C_1 to C_8 of the cable mode shapes as well as its formulation of the n^{th} complex eigenfrequency ω_n can be determined by satisfying the boundary conditions at the cable ends and continuity conditions at the damper location $y = a$. The result of eigenfrequency formula is shown as

$$\frac{\Psi_1\kappa + \Psi_2(1-\kappa)}{\Psi_3\kappa + \Psi_4(1-\kappa)} = \frac{F_{NSD}}{\tilde{v}_a EI} \tag{16}$$

in which κ is the boundary condition index with $\kappa = 0$ for a hinged-hinged end cable and $\kappa = 1$ for a fixed-fixed end cable, respectively.

$$\Psi_1 = 2\delta_1\delta_2(\delta_1^2+\delta_2^2)\{2\delta_1\delta_2[1-\cos(\delta_2 l)\cosh(\delta_1 l)] + (\delta_1^2-\delta_2^2)\sin(\delta_2 l)\sinh(\delta_1 l)\} \tag{17}$$

$$\Psi_2 = 2EI^2\delta_1\delta_2(\delta_1^2+\delta_2^2)^3\sin(\delta_2 l)\sinh(\delta_1 l) \tag{18}$$

$$\begin{aligned}\Psi_3 = {} & \delta_1^3[\cos\delta_2 l - \cos\delta_2(2a-l)]\sinh\delta_1 l + \delta_1^2\delta_2\sin\delta_2 l[3\cosh\delta_1 l + \cosh\delta_1(2a-l)] \\ & -4\delta_1^2\delta_2[\sin(\delta_2 a)\cosh(\delta_1 a) - \sin\delta_2(a-l)\cosh\delta_1(a-l)] \\ & -\delta_1\delta_2^2[3\cos\delta_2 l + \cos\delta_2(2a-l)]\sinh\delta_1 l \\ & +4\delta_1\delta_2^2[\cos\delta_2 a\sinh\delta_1 a - \cos\delta_2(a-l)\sinh\delta_1(a-l)] \\ & -\delta_2^3\sin\delta_2 l[\cosh\delta_1 l - \cosh\delta_1(2a-l)]\end{aligned} \tag{19}$$

$$\begin{aligned}\Psi_4 = {} & EI^2(\delta_1^4+\delta_2^4)\begin{bmatrix}\delta_2\cosh(\delta_1 l)\sin(\delta_2 l) + \delta_1\cos(\delta_2 l)\sinh(\delta_1 l) \\ -\delta_2\sin(\delta_2 l)\cosh\delta_1(2a-l) - \delta_1\sinh(\delta_1 l)\cos\delta_2(2a-l)\end{bmatrix} \\ & -2EI^2\delta_1^2\delta_2^3\sin\delta_2 l[\cosh\delta_1(2a-l) - \cosh(\delta_1 l)] \\ & +2EI^2\delta_1^3\delta_2^2\sinh(\delta_1 l)[\cos(\delta_2 l) - \cos\delta_2(2a-l)]\end{aligned} \tag{20}$$

The complex frequencies ω_n of the cable vibration can be determined by solving eq. (16) directly. These frequencies are complex in which the imaginary component represents the modal damping ratio [5] as

$$\omega_n = |\omega_n|(\sqrt{1-\xi_n^2} + \xi_n i) \tag{21}$$

where ξ_n is the damping ratio of the n^{th} mode; and $|\omega_n|$ is the frequency magnitude of the n^{th} mode. After obtaining ω_n from eq. (16), the damping ratio ξ_n can be deduced using eq. (21) as

$$\xi_n = \frac{\mathrm{Im}[\omega_n]}{|\omega_n|} \tag{22}$$

3.1. Asymptotic Approach

The purpose of the asymptotic solution is to approximate such trigonometric and hyperbolic functions appeared in eq. (16), which will result in an explicit form of ω_n. The added damping ratio then can be deduced from eq. (22). This asymptotic approach assumes that the perturbation of the wave numbers $\Delta\beta_n$ between a flexural cable with a damper and a nonflexural cable without a damper is relatively small. Referring to the author's previous publications for the details of asymptotic solution [14, 15]. As a result of the approximation of Eq. (16), the asymptotic complex frequency formula is subsequently derived as

$$\tan(\beta_n l) = \beta_{tn} l \left(\frac{a}{l}\right) \frac{\Psi_5 \kappa + \Psi_6 (1-\kappa)}{\Psi_7 \kappa + \Psi_8 (1-\kappa)} \tag{23}$$

where $\beta_n = \omega_n \sqrt{m/T}$ = wave number; $\beta_{tn} = n\pi/l$ = wave number of taut-string cable.

$$\Psi_5 = \frac{2}{r} + \frac{F_{NSD} a}{T \tilde{v}_a}\left(1 - \frac{2}{r^2} + \frac{2+2r}{r^2 e^r}\right); \text{ and } \Psi_6 = \left(\frac{2r F_{NSD}}{\tilde{v}_a}\right)\left(\frac{Ta^3}{2r^3}\right) \tag{24a,b}$$

$$\Psi_7 = 1 + \frac{F_{NSD} a}{T \tilde{v}_a}\left(1 - \frac{3}{2r} - \frac{1-4e^r}{2r e^{2r}}\right); \text{ and } \Psi_8 = \left(\frac{Ta^3}{2r^3}\right)\left[\frac{2rT}{a} + \frac{F_{NSD}}{\tilde{v}_a}\left(\frac{1-e^{2r}}{e^{2r}} + 2r\right)\right] \tag{25a,b}$$

On making use of eq. (23), damping ratio can be derived from eq. (22) as

$$\frac{\xi_n}{(a/l)} = \frac{\mathrm{Im}[\omega_n]}{|\omega_n|(a/l)} = \frac{\mathrm{Im}[\beta_n]}{|\beta_n|(a/l)} \simeq \frac{\mathrm{Im}[\tan(\beta_n l)]}{|\beta_{tn} l|(a/l)} = \mathrm{Im}\left[\frac{\Psi_5 \kappa + \Psi_6 (1-\kappa)}{\Psi_7 \kappa + \Psi_8 (1-\kappa)}\right] \tag{26}$$

Substitution of the damper force F_{NSD} from eq. (9) into eq. (26) results in the modal damping ratio as

$$\frac{\xi_n}{(a/l)} = R_2 R_1 \frac{\eta_2 \eta_1 \varphi \bar{K}}{(1 + \eta_2 \eta_1 \bar{K})^2 + (\eta_2 \eta_1 \varphi \bar{K})^2} \tag{27}$$

The maximum modal damping ratio and its optimal damper coefficient as

$$\frac{\xi_n^{\max}}{(a/l)} = 0.5 R_2 R_1 R_\varphi \text{ at } \bar{K}_{opt} = \frac{1}{\eta_2 \eta_1 \eta_\varphi} \tag{28a,b}$$

in which $\eta_1 = [1 - q + (0.5 - \kappa) r q^2]$ and $R_1 = (1 - q\kappa)^2/\eta_1$ are the modification factors of the damper coefficient and its damping ratio due to cable bending stiffness associated with types of boundary conditions at cable ends (κ = 0 for hinged-hinged ends, and κ = 1 for fixed-fixed ends); $q = (1 - e^{-r})/r$; $r = a/(l\sqrt{\eta})$; $\eta_\varphi = \sqrt{1+\varphi^2}$; $R_\varphi = \varphi/(1 + \sqrt{1+\varphi^2})$; η_2 and R_2 are the modification factors of the damper coefficient and its damping ratio due to the negative stiffness, which are defined as

$$R_2 = \frac{1}{\eta_1 \bar{K}_{NS}+1}; \text{ and } \frac{1}{\eta_2} = \eta_1 \bar{K}_{NS} + 1 \quad (29a,b)$$

The allowable range of the dimensionless negative stiffness values $\bar{K}_{NS}$ is determined based on mathematical conditions that the modification the factors R_2 and η_2 must be positive. From which,

$$\frac{-1}{\eta_1} < \bar{K}_{NS} < 0 \quad (30)$$

The complex eigenfrequencies by exact solution eq. (16) and by asymptotic solutions eq. (23) are normalized and plotted with different values of the negative stiffness. The results are shown in Fig. 3 for fixed-fixed end cable and Fig. 4 for hinged-hinged end cable, respectively.

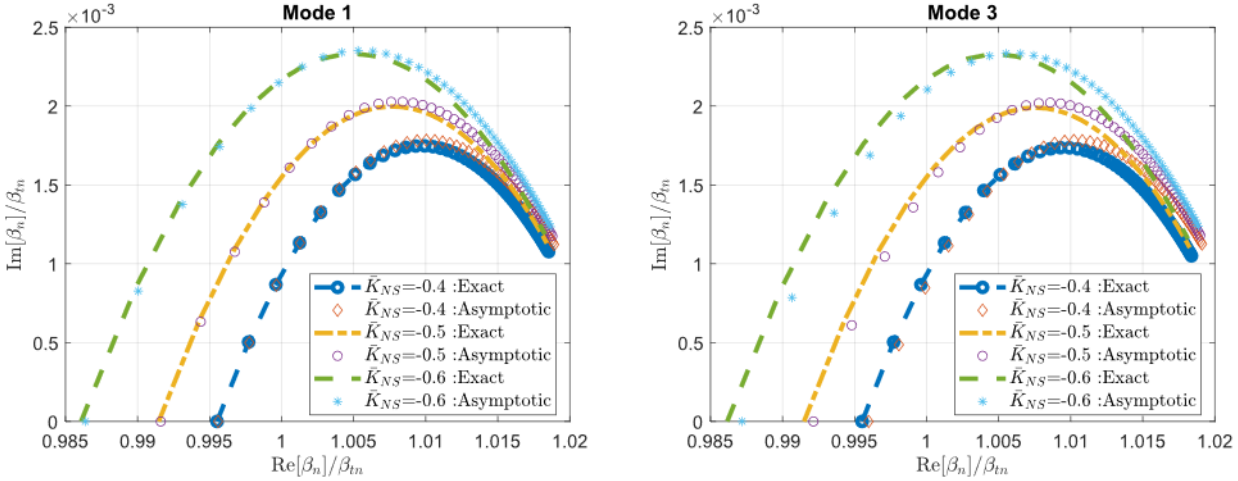

Figure 3. Complex wave number with different negative stiffness $\bar{K}_{NS}$ for fixed-fixed end cable.

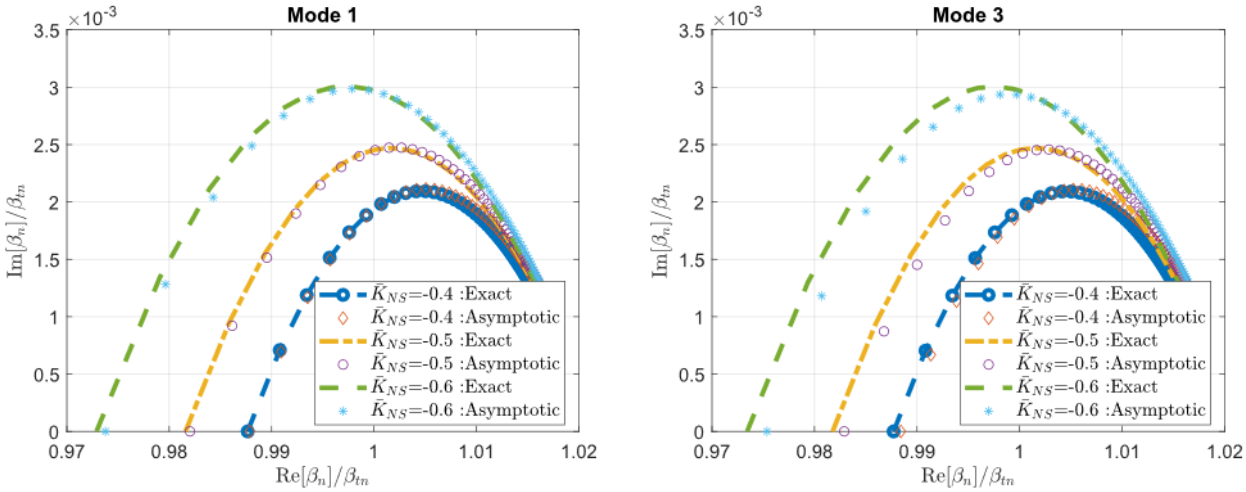

Figure 4. Complex wave number with different negative stiffness $\bar{K}_{NS}$ for hinged-hinged end cable.

Figs. 3 and 4 show a good agreement between the exact and asymptotic solution. The discrepancies between the exact solution and asymptotic solution are characterized by $\Delta\beta_n$. Figs 3 and 4 pointed out that the increase in the negative stiffness caused the decrease in the wave number and its cable frequency accordingly. Consequently, a cable-damper system will be

unstable in the existence of negative stiffness if the natural frequencies of cables approach to zero.

3.2. Numerical Approach by Finite Difference Method (FDM)

In addition to the presented asymptotic approach, a numerical solution by the FDM is developed in this section as a parallel solution for the verification of the proposed damping formulation. A cable with a length l is discretized into N elements along the cable with n internal nodes ($n = N - 1$). Each element has an equal length of a_1. Cable natural frequencies and its damping ratios can be determined by solving the subsequent matrix formulation.

$$[K]\{\tilde{v}\} + p[C]\{\tilde{v}\} + p^2[M]\{\tilde{v}\} = 0 \tag{31}$$

where $[K]$, $[C]$ and $[M]$ are the stiffness, damping and mass matrices of the discretized cable; $\tilde{v}$ is the mode shape vector of nodal displacements; $p = -\xi\omega_0 \pm i\omega_0\sqrt{1-\xi^2}$ is the complex number related to the damping ratio ξ and undamped natural circular frequency ω_0. These matrices have size of $n \times n$. Since this section aims to verify the proposed damping formula in the preceding section, the matrices appeared in eq. (31) will be modified to contain only characteristics of a stay cable attached by a NS-HDR damper. For that purpose, $[C]$ is a zero matrix since the inherent damping is relatively small and neglected. Mass matrix $[M]$ as

$$[M] = \text{diag}\{m_1, m_2, \ldots, m_n\} \tag{32}$$

where m_i is the mass per unit length at node i. Stiffness matrix $[K]$ as

$$[K] = [K_1] + [K_2] \tag{33}$$

where $[K_1]$ is the stiffness matrix due to cable bending stiffness EI and static cable tension T; and $[K_2]$ is the stiffness matrix due to NS-HDR damper. Stiffness matrix $[K_1]$ as

$$[K_1] = \frac{T}{a_1^2}\left(\frac{1}{\lambda^2}\right)\begin{bmatrix} \alpha n^2 + 2\lambda^2 & -4n^2 - \lambda^2 & n^2 & 0 & 0 & 0 & 0 & 0 \\ -4n^2 - \lambda^2 & 6n^2 + 2\lambda^2 & -4n^2 - \lambda^2 & n^2 & 0 & 0 & 0 & 0 \\ n^2 & -4n^2 - \lambda^2 & 6n^2 + 2\lambda^2 & -4n^2 - \lambda^2 & n^2 & 0 & 0 & 0 \\ 0 & n^2 & -4n^2 - \lambda^2 & 6n^2 + 2\lambda^2 & -4n^2 - \lambda^2 & n^2 & 0 & 0 \\ 0 & \cdots & \cdots & \cdots & \cdots & \cdots & \cdots & 0 \\ 0 & 0 & 0 & 0 & n^2 & -4n^2 - \lambda^2 & 6n^2 + 2\lambda^2 & -4n^2 - \lambda^2 \\ 0 & 0 & 0 & 0 & 0 & n^2 & -4n^2 - \lambda^2 & \alpha n^2 + 2\lambda^2 \end{bmatrix} \tag{34}$$

where $\lambda^2 = Tl^2/EI$; and α is the boundary condition index (7 or 5 for fixed ends or hinged ends, respectively). In this study, because a negative stiffness HDR damper is installed to the cable at the damper location, the stiffness matrix $[K_2]$ will contain only one non-zero element corresponding to the node where the negative stiffness HDR damper is mounted to the cable.

From which,

$$[K_2] = \text{diag}\{0,0,\ldots,K_{eq}(1 + \varphi_{eq}i)/a_1,\ldots,0\} \tag{35}$$

After having these matrices available, eq. (31) can be solved and the damping ratio ξ will be obtained accordingly.

$$\xi = \frac{-\mathrm{Re}[p]}{\sqrt{(\mathrm{Re}[p])^2 + (\mathrm{Im}[p])^2}} \tag{36}$$

Comparisons between the asymptotic solution and FDM about the natural frequencies and damping ratios in some real cables are presented. The cable properties and damper characteristics are shown in Table 1. Table 2 shows the natural frequencies and damping ratios for the fixed-fixed end cables while Table 3 shows the results for the hinged-hinged end cables. In both tables, the natural frequencies and damping ratios by the proposed asymptotic solution agreed well with the results by the FDM, with an error of 2% on average for damping ratios and less than 1% for frequencies.

Table 1. Cable properties and damper characteristics.

Cable No.	Cable properties				Negative stiffness HDR Damper			
	Cable length l (m)	Mass per unit length m (kg/m)	Bending stiffness EI (N.m^2)	Tension T (N)	Damper location a (m)	Spring factor K (N/m)	Loss factor φ	Negative stiffness K_{NS} (N/m)
C1	137.82	68.4	2.73×10^6	3.45×10^6	4.54	644×10^3	0.62	-300×10^3
C2	127.47	68.4	2.73×10^6	4.26×10^6	4.37	644×10^3	0.62	-300×10^3
C3	167.18	64.3	2.34×10^6	3.10×10^6	5.54	563×10^3	0.62	-300×10^3
C4	184.72	60.2	1.98×10^6	3.20×10^6	5.85	483×10^3	0.62	-300×10^3
C5	167.18	64.3	2.34×10^6	3.18×10^6	5.54	563×10^3	0.62	-300×10^3
C6	184.72	60.2	1.98×10^6	3.67×10^6	5.85	483×10^3	0.62	-300×10^3

Table 2. Comparisons between asymptotic solution and FDM for fixed-fixed end cables.

Cable No.	Asymptotic solution				Finite Difference Method (FDM)					
	Frequency f (Hz)			Damping ratio ξ (%)	Frequency f (Hz)			Damping ratio ξ (%)		
	f_1	f_2	f_3	$\xi_1 = \xi_2 = \xi_3$	f_1	f_2	f_3	ξ_1	ξ_2	ξ_3
C1	0.834	1.667	2.500	0.596	0.833	1.668	2.504	0.595	0.596	0.596
C2	0.999	1.997	2.996	0.563	0.999	1.998	3.000	0.559	0.558	0.557
C3	0.671	1.341	2.011	0.708	0.671	1.342	2.014	0.743	0.745	0.747
C4	0.635	1.269	1.904	0.723	0.634	1.269	1.904	0.721	0.721	0.721
C5	0.679	1.358	2.037	0.704	0.679	1.359	2.040	0.739	0.740	0.739
C6	0.679	1.358	2.037	0.688	0.679	1.358	2.037	0.684	0.684	0.683

Table 3. Comparisons between asymptotic solution and FDM for hinged-hinged end cables.

Cable No.	Asymptotic solution				Finite Difference Method (FDM)					
	Frequency f (Hz)			Damping ratio ξ (%)	Frequency (Hz)			Damping ratio ξ (%)		
	f_1	f_2	f_3	$\xi_1 = \xi_2 = \xi_3$	f_1	f_2	f_3	ξ_1	ξ_2	ξ_3
C1	0.827	1.653	2.480	0.784	0.826	1.653	2.482	0.780	0.782	0.784
C2	0.990	1.980	2.970	0.746	0.989	1.980	2.972	0.737	0.738	0.738
C3	0.666	1.332	1.999	0.867	0.666	1.333	2.001	0.898	0.900	0.905
C4	0.631	1.262	1.893	0.875	0.631	1.262	1.893	0.869	0.869	0.871
C5	0.675	1.349	2.024	0.862	0.675	1.350	2.026	0.892	0.894	0.899
C6	0.675	1.351	2.026	0.830	0.675	1.350	2.025	0.822	0.822	0.822

The investigation into the effect of a NS-HDR damper on the increase in the added damping was subsequently implemented, in which a cable with properties $T = 3 \times 10^6$ N, $l = 100$ m, and $m = 78.3$ kg/m was used. A NS-HDR damper with the material loss factor $\varphi = 0.25$ was transversely attached to cable at the location $a/l = 0.02$. Figs. 5(a)-(b) investigates the damping curves versus the HDR damper coefficient $\overline{K}$ for a fixed end cable with small bending stiffness ($\eta = 1 \times 10^{-6}$) and large bending stiffness ($\eta = 1 \times 10^{-4}$), respectively.

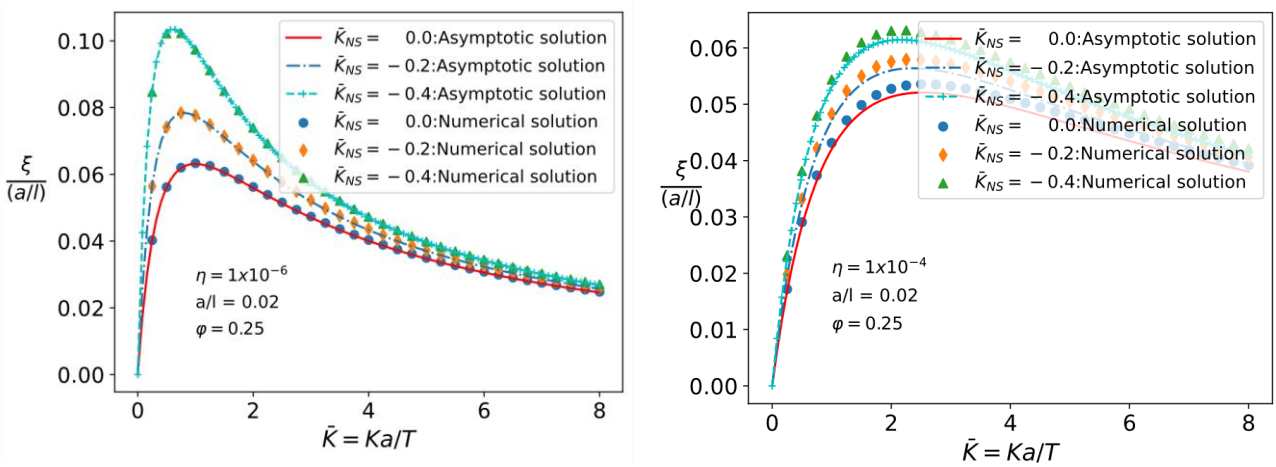

(a) (b)

Figure 5. Damping curves with different values of $\bar{K}_{NS}$ for a flexural cable with fixed ends: (a) small bending stiffness ($\eta = 1 \times 10^{-6}$); and (b) large bending stiffness ($\eta = 1 \times 10^{-4}$).

As they appeared, the modal damping ratio calculated by the asymptotic solution matched well with those by the numerical approach, holding the threshold discrepancies of 2.3 % and 3.1% for a small and lager bending stiffness cable, correspondingly. Compared to a conventional HDR damper ($\bar{K}_{NS}$ = 0), a negative stiffness HDR damper ($\bar{K}_{NS}$ < 0) generated superior supplemental damping to the cable. The comparisons about damping ratios between a nonflexural cable, flexural cable with fixed ends and flexural cable hinged ends were also investigated and plotted in Fig. 6

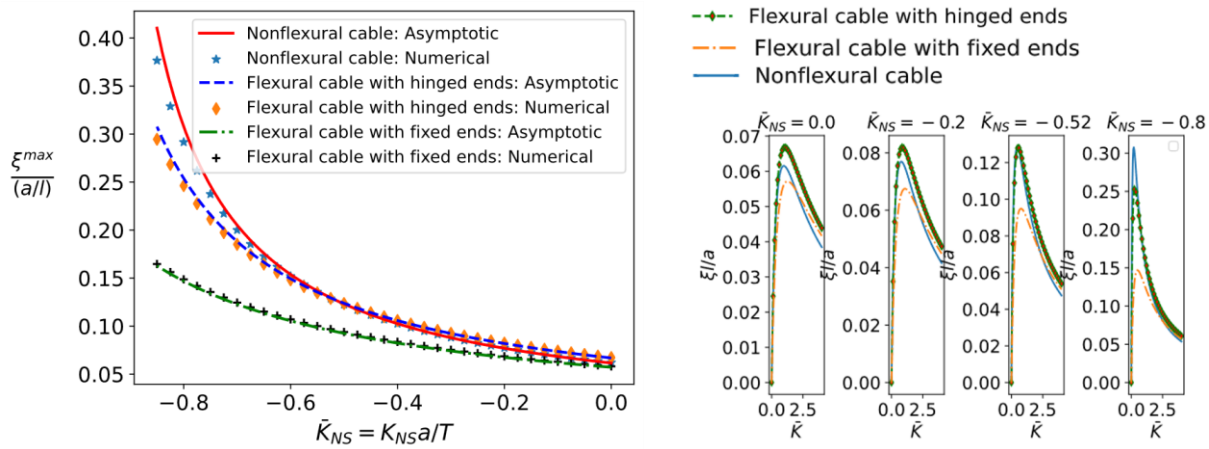

(a) (b)

Figure 6. Comparison of the maximum damping ratios between a nonflexural cable, flexural cable with fixed ends and hinged ends.

As can be seen in Fig. 6, the increase in the negative stiffness $\bar{K}_{NS}$ (more negative) led to an increase in the maximum added damping ratio, and this increase was much faster for a nonflexural cable than that of a flexural cable. Moreover, the increase in the negative stiffness $\bar{K}_{NS}$ (more negative) also resulted in larger discrepancies about damping between these three cable models.

4. A CASE STUDY

This section aims to demonstrate the design of the NS-HDR damper for a targeted set of cables belonging to an existing cable-stayed bridge. The bridge has a length of 600 m, and the cable lengths vary from 100 m to 200 m, with the height of the main towers around 127 m. To mitigate cable vibrations, HDR dampers were already attached to the cables of the bridge. Fig. 7 provides an overview of the bridge, highlighting the cables chosen for the design example. The properties of these selected cables are summarized in Table 4 and a flowchart of design is displayed in Fig. 8.

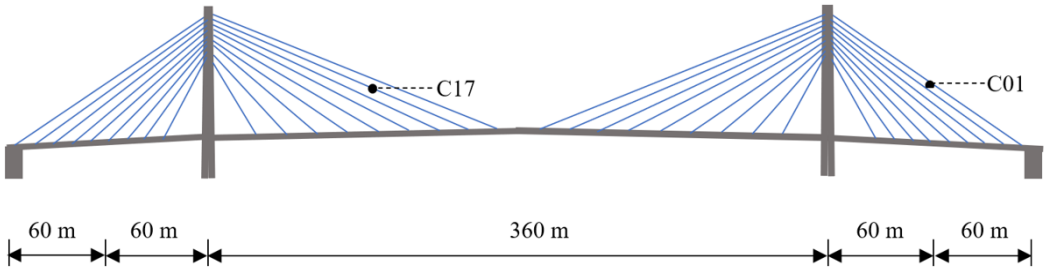

Figure 7. The bridge layout.

Table 4. Properties of the selected cables and attached HDR damper.

Cables	*Cables*				*HDR damper*		
	l **(m)**	***m*** **(kg/m)**	***EI*** **(N.m^2)**	***T*** **(N)**	***a (m)***	***K (N/m)***	***φ***
C01	137.82	68.40	2.73E+06	3.57E+06	4.54	6.44E+05	0.62
C17	167.18	64.30	2.34E+06	3.34E+06	5.54	5.63E+05	0.62

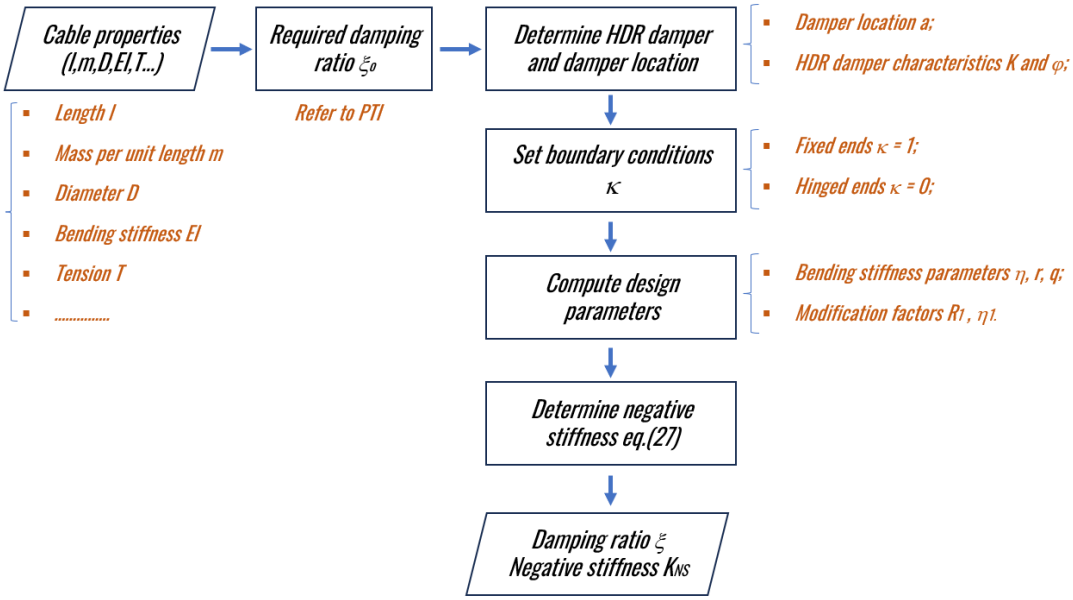

Figure 8. Flowchart of NS-HDR damper design.

In order to determine the necessary parameters for NS-HDR damper design, full-scale measurements of cable vibrations were presented as a design example. Vibration data were sampled by the accelerometers at a sampling frequency of 1000 Hz. The transducer was strategically placed at 7.719 m from the anchor for cable C01 and 8.797 m for cable C17. The

chosen excitation method involved using a rope to pull and release, creating a controlled and repeatable excitation for the cables. The fundamental natural frequency and damping of the cables were extracted from the vibration signals. Fig. 9 displays the raw vibration data of the cables. The determination of cable natural frequency and cable damping ratio involves four steps, as illustrated in Fig. 10, using the measured vibration data.

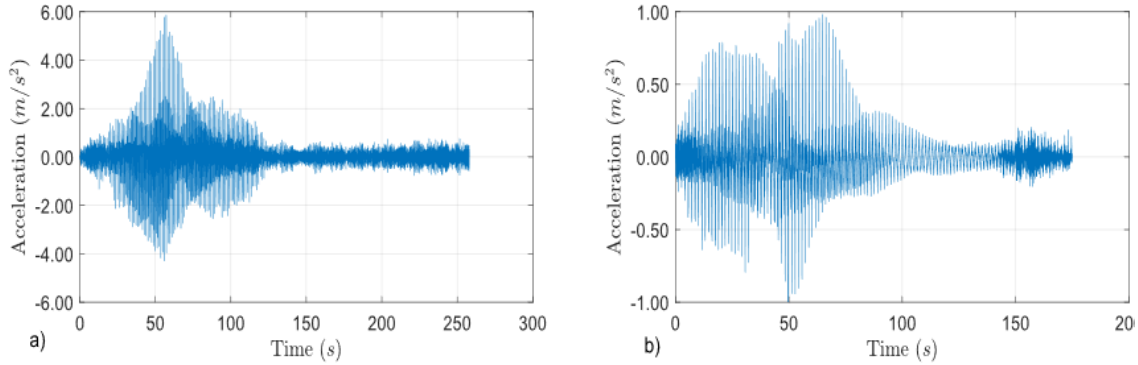

Figure 9. Raw cable acceleration data: a) Cable C01; b) Cable C17.

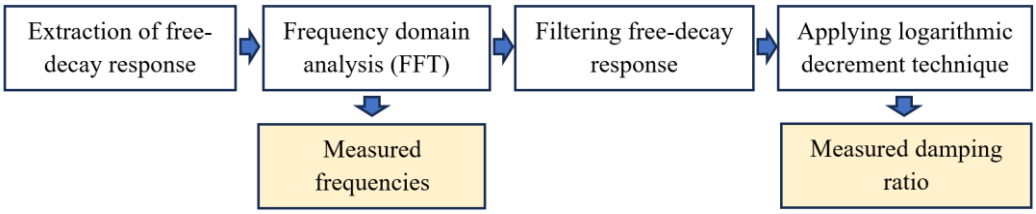

Figure 10. Procedures for the determination of measured frequency and measured damping.

The first step is to extract the free-decay response from measured vibrations. The second step involves performing spectrum analysis in the frequency domain (frequency domain analysis). In this step, the free vibration in the time domain is transformed into the frequency domain using Fast Fourier Transform (FFT) analysis [16]. The measured natural frequencies of cables are then extracted from the prominent peaks of the frequency spectrum. Fig. 11 displays the frequency domain analysis results of the measured data for cables C01 and C17 using FFT analysis. The third step is to filter free-decay response. A bandpass Butterworth filter [17] is used to eliminate noise and to disregard unwanted vibration modes from the raw data. The last step is to determine measured damping ratio using the natural logarithm graph [18] of the decay amplitudes.

$$\xi \approx \frac{\delta}{2\pi} = \frac{1}{2\pi j} \ln\left|\frac{A_\Theta}{A_{\Theta+j}}\right| \tag{37}$$

where A_Θ and $A_{\Theta+j}$ are the amplitudes of the filtered free-decay responses at the Θ and $\Theta + j$ peaks, respectively; and δ is the logarithmic decrement. Fig. 12 shows filtered free-decay responses of the cables C01 and C17, and damping ratio is obtained from the decay curve of the response. As a result, Table 5 summarizes the measured cable damping and measured cable natural frequencies.

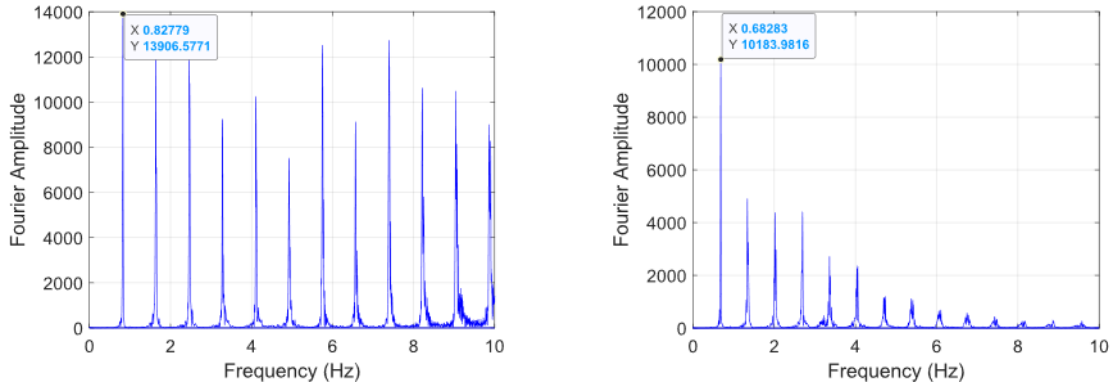

a) b)

Figure 11. Frequency identification using FFT: a) cable C01; b) cable C17.

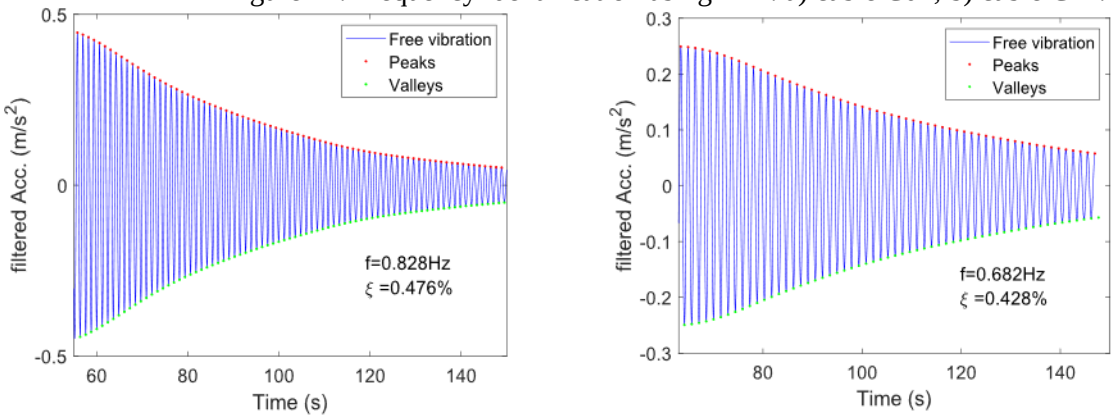

a) b)

Figure 12. Damping identification: a) cable C01; b) cable C17.

Table 5. Measured natural frequency and measured damping ratio ξ of the cables.

Cables	**1st Natural frequency f (Hz)**	**1st Damping ratio ξ (%)**
C01	0.828	0.476
C17	0.682	0.428

Table 6. Design of NS-HDR damper.

Cable	Input							Output
	Required damping ξ (%)	(a/l)	κ	η	η_1	R_1	$\bar{K}$	Negative stiffness K_{NS} (kN/m)
C01	0.5	0.033	1.0	4.17×10^{-5}	0.708	0.915	0.847	−160.0
C17	0.5	0.033	1.0	2.64×10^{-5}	0.768	0.930	0.984	−90.9

The measured damping ratios of cable C01 and C17 are 0.48% and 0.43%, respectively. However, according to PTI[4], a damping ratio between 0.5% and 1.0% would be sufficient to suppress rain-wind induced vibrations. The current HDR damping, in fact, provides damping less than 0.5%. Therefore, the NS-HDR damper proposed in this study will be designed to achieve the required damping of 0.5%. The purpose of this case study is to determine the negative stiffness value that needs to be added to the current HDR damper to create NS-HDR damper, which will generate a damping value of 0.5%. For this purpose, the proposed damping formulation, eq. (27), is used, and the results are summarized in Table 6. The table shows that a

negative stiffness of 160 kN/m and 90.9 kN/m should be installed to the current HDR damper to achieve the desired 0.5% damping for cables C01 and C17, respectively.

In this example, the negative stiffness component is specifically engineered to increase the added damping ratio to 0.5%. Within the NS-HDR damper model, it's crucial to emphasize that the damping ratio remains consistent across all vibration modes for cable model without sag consideration. In simpler terms, the additional damping supplied by the NS-HDR damper in the 2nd and 3rd modes is identical to that in the 1st mode, ensuring uniform damping across all modes.

5. CONCLUSIONS

The contributions and prominent points obtained throughout this study are as follows:

- An explicit formulation of the modal damping ratio for a stay cable with a NS-HDR damper are derived for a flexural cable with fixed-fixed ends or hinged-hinged ends. The effect of negative stiffness on the damping ratio is presented through a proposed modification factor. This factor means the modification of the added damping compared to the conventional HDR damper.
- In the presence of negative stiffness, the NS-HDR damper generates superior added damping to the cable. For cables with the same boundary conditions, the small bending stiffness cables received more benefit from negative stiffness than that of the large stiffness cables. For cables with the same flexural rigidity but different boundary conditions, the hinged-hinged end cables pose higher damping than that of the fixed – fixed end cables.
- The increase in negative stiffness leads to an increase in the achievable damping, and this damping increment is much faster for a nonflexural cable (taut-string cable) than that of a flexural cable.
- A NS-HDR damper yields a peak on the damping curve which is always shifted to the left-hand side of an original peak, leading to a smaller size of the designed HDR damper (smaller spring factor K). The original peak means the peak of the damping curve corresponding to a conventional HDR damper without negative stiffness.
- A numerical solution by the Finite Difference Method (FDM) is introduced to verify the analytical damping formula. It showed a good agreement between the two approaches.
- As a practical example, a case study was presented, focusing on the damping of cables (137.82m and 167.18m in length), where the measured damping ratios were found to be smaller than 0.5%. To address this issue, the NS-HDR damper has been specifically designed for these cables to achieve the desired damping ratio of 0.5%.

ACKNOWLEDGMENT

This research is funded by University of Transport and Communications (UTC) under grant number T2023-CT-013. The authors thank Structural Lab of Yokohama National University in Japan for supporting this study

REFERENCES

[1] Y. Fujino, N. Hoang, Design formulas for damping of a stay cable with a damper, J. Struct. Eng., 134 (2008) 269-278. https://doi.org/10.1061/(ASCE)0733-9445(2008)134:2(269

[2] B.M. Pacheco, Y. Fujino, A. Sulekh, Estimation curve for modal damping in stay cables with viscous damper, J. Struct. Eng., 119 (1993) 1961-1979. https://doi.org/10.1061/(ASCE)0733-9445(1993)119:6(19

[3] N.J. Gimsing, C.T. Georgakis, Cable supported bridges: Concept and design, John Wiley & Sons, 2011.

[4] PTI, Recommendations for stay cable design, testing and installation, in, Cable-Stayed Bridges Committee Phoenix, 2007.

[5] S. Krenk, Vibrations of a taut cable with an external damper, J. Appl. Mech., 67 (2000) 772-776. https://doi.org/10.1115/1.1322037

[6] J. Main, N. Jones, Free vibrations of taut cable with attached damper. II: Nonlinear damper, J. Eng. Mech., 128 (2002) 1072-1081. https://doi.org/10.1061/(ASCE)0733-9399(2002)128:10(107

[7] J. Main, N. Jones, Free vibrations of taut cable with attached damper. I: Linear viscous damper, J. Eng. Mech., 128 (2002) 1062-1071. https://doi.org/10.1061/(ASCE)0733-9399(2002)128:10(1062)

[8] H. Tabatabai, A.B. Mehrabi, Design of mechanical viscous dampers for stay cables, J. Bridge Eng., 5 (2000) 114-123. https://doi.org/10.1061/(ASCE)1084-0702(2000)5:2(11

[9] L. Chen, L. Sun, S. Nagarajaiah, Cable with discrete negative stiffness device and viscous damper: passive realization and general characteristics, Smart Struct. Syst., 15 (2015) 627-643. https://doi.org/10.12989/sss.2015.15.3.627

[10] P. Zhou, H. Li, Modeling and control performance of a negative stiffness damper for suppressing stay cable vibrations, Struct Control Health Monit., 23 (2016) 764-782. https://doi.org/10.1002/stc.1809

[11] X. Shi, S. Zhu, J.-Y. Li, B.F. Spencer, Dynamic behavior of stay cables with passive negative stiffness dampers, Smart Mater. Struct., 25 (2016) 075044. https://doi.org/10.1088/0964-1726/25/7/075044

[12] X. Shi, S. Zhu, B.F. Spencer Jr, Experimental study on passive negative stiffness damper for cable vibration mitigation, J. Eng. Mech., 143 (2017) 04017070. https://doi.org/10.1061/(ASCE)EM.1943-7889.00012

[13] M. Javanbakht, S. Cheng, F. Ghrib, Impact of support stiffness on the performance of negative stiffness dampers for vibration control of stay cables, Struct Control Health Monit., 27 (2020) e2610. https://doi.org/10.1002/stc.2610

[14] L.X. Le, H. Katsuchi, H. Yamada, Effect of rotational restraint at damper location on damping of a taut cable with a viscous damper, J. Bridge Eng., 25 (2020) 04019139. https://doi.org/10.1061/(ASCE)BE.1943-5592.0001520

[15] L.X. Le, H. Katsuchi, H. Yamada, Damping of cable with HDR damper accounting for restraint boundary conditions, J. Bridge Eng., 25 (2020) 04020105. https://doi.org/10.1061/(ASCE)BE.1943-5592.0001641

[16] A.K. Chopra, Dynamics of structures, Pearson Education India, 2007.

[17] S. Butterworth, On the theory of filter amplifiers, Wirel. Eng., 7 (1930) 536-541.

[18] S.G. Kelly, Mechanical vibrations: theory and applications, Cengage learning, 2012.